Journal of Power Sources, 6 (1981) 229 - 243

ELECTROCHEMICAL REACTIONS ON SOME CEMENTED METAL CARBIDES

ASHOK K. VIJH, G. BELANGER and R. JACQUES
Institut de Recherche d'Hydro-Québec, Varennes, Que. (Canada)
(Received March 31, 1980; in revised form August 11, 1980)

Summary

The electrochemical behaviour of cobalt-cemented tungsten carbides has been examined in aqueous alkaline solutions. These electrodes exhibit a good surface stability in the potential region *ca.* 0.0 - 0.7 V (*vs.* RHE); the presence of a passivating surface oxide is indicated in this potential range. The anodic oxidation tendencies of a number of organic compounds were explored but only hydrazine underwent oxidation at an appreciable rate.

A detailed mechanistic study on the anodic oxidation of hydrazine has been carried out. The experimental data consist of potentiostatic and potentiodynamic current–potential relationships, reaction order derivatives, apparent heats of activation, and an ellipsometric investigation of the electrode surface. Based on these data and some general considerations, a mechanism is proposed in which the first charge transfer step involving a hydroxyl ion and the molecular residue of hydrazine is the rate-determining step (r.d.s.).

Introduction

One of the central problems in modern electrochemical reseach is the discovery of electrode materials that exhibit suitable electrochemical stability and also possess good electrocatalytic properties towards potentially-useful electrode reactions. To this end, much work bearing on the electrode behavior of diverse materials has appeared in the literature. The present work falls within the general context of such studies.

Cemented hard metal carbides are carbides of tungsten (and/or of titanium and tantalum) in which a transition metal, usually cobalt, is added as a "cementing" material; *e.g.*, by mixing appropriate quantities of powders of WC and Co above a eutectic temperature, a suitable cemented hard metal carbide may be obtained [1]. These materials are usually employed under conditions where high temperature wear resistance is essential.

Our choice of these materials for electrochemical studies was suggested by the facts that carbides show high catalytic activity in the gas phase [2 - 5] and have been found to have adequate electrochemical stability in some

electrolyte media [6, 7]. Also, cobalt is reasonably stable and has good electrocatalytic activity when passivated by an oxide in alkaline solutions [8]. Based on the foregoing observations, we had concluded that cemented metal carbides are perhaps good candidates as possibly stable electrodes possessing significant electrocatalytic activity.

The electrical conductivities of these materials are comparable with those of metals [1] and the starting materials needed for their fabrication are not all that scarce or expensive (*cf.* platinum). The chemical composition of the various electrode materials used in the first preliminary scanning are shown in Table 1. The cemented carbides (electrodes 1 - 4) were stable, after the first "conditioning" potentiostatic curve, in the potential range 0.0 - 0.7 V *vs.* the reversible hydrogen electrode in deoxygenated 1M KOH aqueous solutions. Above the anodic limit of 0.7 V, strong corrosion of cobalt is observed. Similar difficulties regarding electrode stability were also observed at potentials cathodic to 0.0 V, presumably owing to the corrosion of non-passivated cobalt. Pure tungsten showed very high rates of corrosion and anodic dissolution in 1M KOH and was thus not studied from an electrocatalytic point of view. The detailed results to be presented here were obtained on typical electrode materials (electrode # 3 or 4 in Table 1) which gave a corrosion-free passive region between 0.01 and 0.7 V (RHE). Some data obtained on pure WC (*i.e.*, electrode # 5) will also be presented in order to bring out the significance of the results.

Experimental

(a) Cell

A conventional three-compartment Pyrex cell was used for the electrochemical measurements. The compartments were separated by solution-sealed stopcocks and isolated from the ambient atmosphere by water-filled bubblers.

(b) Electrodes

(i) Working electrodes

The cemented tungsten carbide electrodes were made of rods of 1/4 in. dia. purchased from the Canadian General Electric (Carboloy Division). The pure tungsten carbide electrodes (*i.e.*, those without the cementing metal such as Co) were poly-crystalline rods of 1/4 in. dia. procured from Research Organic and Inorganic Chemical Corporation, U.S.A. The working electrodes were mounted in a piece of Kel. F. material and were polished on a rotating wheel covered with a nylon cloth disc, using a 3 micron diamond paste; for the ellipsometric work, the polishing was done with a diamond paste of 1 micron.

The polished electrodes were thoroughly cleaned, degreased and washed with de-ionized and doubly distilled water, the second distillation being over alkaline $KMnO_4$.

TABLE 1

The compositions of electrode materials

Electrode	Composition (%)			
#	WC	TaC	TiC	Co
1	92	4		4
2	71	12.5	12	4.5
3	72	11.5	8	8.5
4	94			6
5	100			

(ii) Auxiliary electrodes

The counter electrodes employed in this study were made from pure tungsten carbide mounted in a piece of heat-shrinkable Teflon tubing.

(iii) Reference electrode

The reference electrode was an Hg/HgO electrode in 1M KOH solution and was fabricated in our laboratory. The contact junction with the electrolyte solution was made by a plug made from alumina paper (type APA-2) obtained from Zircar Products Inc., New York, U.S.A. The potential of this electrode was checked against a hydrogen electrode in the same solution and found to be 0.926 volts.

(c) Solution

The electrolyte was 1M KOH solution made up from de-ionized, doubly distilled water, the second distillation being over alkaline $KMnO_4$. The KOH was ACS reagent grade and was obtained from the Fisher Scientific Company, Fairlawn, N.Y., U.S.A. The various chemicals whose oxidation was examined in this study (*e.g.*, hydrazine, ethylene glycol, potassium acetate, etc.) were purchased either from Fisher Chemical, from Eastman Chemicals (a division of Eastman Kodak Co., Rochester, N.Y., U.S.A.) or other similar reliable sources (*e.g.*, ICN Pharmaceuticals Inc., Plainview, N.Y., U.S.A.) and were ACS reagent grade or the purest available. The solution in the cell was deoxygenated by bubbling helium through the working and the auxiliary compartments. All measurements were carried out in helium-stirred solutions.

(d) Instruments and measurement

(i) Potentiostatic measurement

The potentiostatic polarisation circuit consisted of a Tacussel potentiostat (PRT-20-2B), in conjunction with a Tacussel Servovit and a cam gear timer. The Servovit fixed the upper and lower limits of the potential and the pilot voltage was driven by the cam gear timer in steps of 8 mV/2 min, in order to obtain a point-by-point steady-state current potential relationship.

(ii) Potentiodynamic circuit

The Tacussel potentiostat (PRT-20-2B) and a Tacussel Function Generator were used together with a Hewlett-Packard X–Y recorder.

(iii) Ellipsometric studies

The ellipsometer used was a Thin Film Ellipsometer Type 43603-200E Ser.no. 5004, purchased from Rudolph Research, Fairfield, N.Y., U.S.A.; it was used in combination with the RR-2000 automatic attachment. The current–potential results were followed on an H.P. 7004-B X–Y recorder; these data were also simultaneously recorded on a magnetic tape recorder (Kennedy Model 9800) together with the corresponding ellipsometric readings for the azimuth (α), intensity (I_{av}) and ellipticity (ϵ).

Results

(a) Preliminary screening

In any work on electrocatalysis and the mechanism of electrode reactions, it is imperative to examine the electrochemical stability of the electrode first. In our preliminary screening of the experimental conditions under which a relative stability of the electrode surface might be achieved, it was found that cemented metal carbides show virtually no current ($\ll 1\ \mu A\ cm^{-2}$) in the current–potential relationships in the electrode polarization range *ca.* 0 - 0.7 V (RHE) in 1M KOH solutions. Occasionally, a small peak (*ca.* 1 - 2 $\mu A\ cm^{-2}$) was observed on a freshly polished electrode during the first potentiostatic curve; this peak could not always be reproduced and, in any case, disappeared after the first polarization curve. In all subsequent curves, no corrosion currents were observed and the results to be presented below refer to these stable surfaces, presumably covered by an oxide since the polished electrodes acquired a slightly dull appearance. This point will be examined further in the Section on ellipsometric studies.

As mentioned earlier, the electrode stability was poor outside the potential range 0.0 - 0.7 V (RHE). However, by comparison with platinum and other catalytic metals, it would appear that this rather restricted potential range is, nevertheless, sufficiently satisfactory for the investigation of the anodic oxidation of some organic molecules.

In the preliminary survey on the oxidation of organic molecules on electrode materials # 3 - 5 (see Table 1), it was found that hydrazine undergoes a facile oxidation on cobalt cemented carbides but not on the WC itself (Table 2). A high activity for the anodic oxidation of hydrazine on cemented metal carbides suggested that other compounds containing $-NH_2$ groups might also undergo significant oxidation. Virtually no oxidation currents were observed for acetamide and guanidine. On the other hand, solutions containing biguanide exhibited high anodic currents on cemented metal carbides, but these currents were vitiated by the visible filming of the electrode by a yellow precipitate and the evident high corrosion of the electrode. In

TABLE 2

Activity at 0.6 V (RHE) $\mu A\ cm^{-2}$

Oxidant (1M)	Electrode #		
	3	4	5
Nil (KOH)	Nil	Nil	Nil
Methanol	Nil	Nil	Nil
Ethylene glycol	<1		
Potassium formate	Nil		
Potassium acetate	Nil		
Potassium perfluoroacetate	Nil		
Urea	Nil		
Acetamide	0.8		
Hydrazine	320	160	<1
Guanidine $HNC(NH_2)_2$	Nil		
Biguanide $H_2NCNH\ CNH_2$ (N H, N H)	40	80	

the light of the results of this preliminary screening (Table 2) detailed mechanistic studies were conducted on the anodic oxidation of hydrazine only, as below.

(b) Current–potential relationships

In the "steady state", point-by-point (in steps of 8 mV/2 min) current–potential relationships obtained potentiostatically, inhibition inflexions characteristic of the anodic oxidation of organic materials [9] are observed on cemented carbides. The inhibition inflexions are more pronounced on the ascending (on the potential scale) curve but are also noted on the descending curve (Fig. 1). These inhibition curves are a form of electrode passivation caused either by surface oxide formation or the deposition of strongly chemisorbed intermediates produced during oxidation of the organic molecule such as the hydrazine [10]. At higher anodic potential, *ca.* >0.4 V *vs.* RHE, a Tafel region is observed; the Tafel slope for the descending line is 113 mV/decade, but somewhat higher for the ascending curve, although still not far removed from $2.3 \times 2RT/F$. Below 0.1 V on the ascending curve, a sort of loop is observed which cannot be given an interpretative significance since the concomitant occurrence of some electrode corrosion, some surface oxide formation, possible reduction of this oxide by the adsorbed hydrogen produced by the dissociative chemisorption of hydrazine and some background redox reactions, etc. ..., can complicate matters beyond interpretation.

In Fig. 1 one may also note a central new contribution to the literature on electrocatalysis brought out by the present study: the activity of pure WC (curve A in Fig. 1) is vanishingly small by comparison with the activity of WC cemented by cobalt (curve B). It confirms the reasoning behind our choice of electrode materials (see the Introduction), namely, that a small

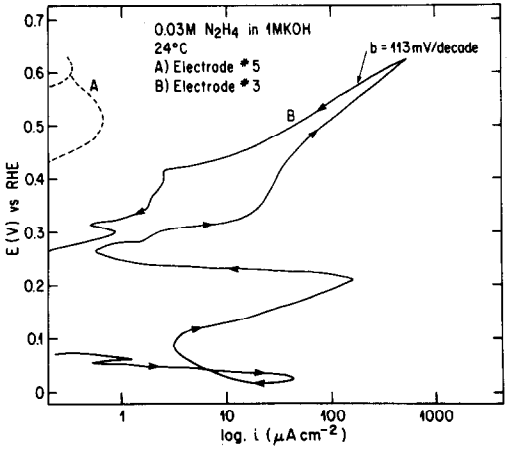

Fig. 1. Potentiostatic potential–log (current density) relationships on pure WC (electrode # 5) and a cobalt-cemented carbide electrode (electrode # 3) in the ascending and the descending directions of potentials; potential interval steps are 8 mV/2 min.

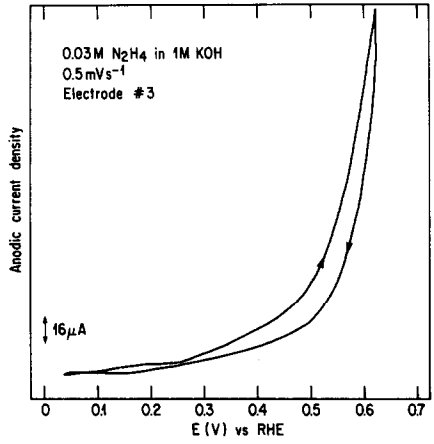

Fig. 2. A typical potentiodynamic profile on cobalt-cemented tungsten carbide; see Table 1 for electrode composition.

amount of transition metal, such as cobalt, should impart high electrocatalytic activity (by analogy with the case of heterogeneous catalysis in the gas phase) provided that the electrode surface can be stabilised against corrosion as, *e.g.*, by the formation of a surface oxide. Mention may be made here of a previous claim regarding the activity of pure WC for hydrazine oxidation; this work [10a] was, however, carried out on porous electrodes under non-steady-state conditions.

In Fig. 2, a typical current–potential relation, obtained potentiodynamically on a cemented tungsten carbide (WC = 94%; Co = 6%) in 1M KOH solution containing 0.03M N_2H_4, is shown. It is quite similar to the potentiostatic curves (Fig. 1) in that faradaic current for the oxidation of hydra-

zine is observed with the occurrence of a faradaic "peak" on the ascending curve around 0.22 V, *i.e.*, corresponding to the inhibition inflection in Fig. 1. No pseudo-faradaic peaks corresponding to the deposition and removal of adsorbed intermediates [11] are indicated in these profiles; a similar behaviour was also observed in curves obtained at a series of different sweep rates.

Another important feature of the curves in Fig. 1 (electrode # 3) is the very pronounced hysteresis between the ascending and descending current–potential relationships. This hysteresis is usually indicative of the surface changes in the electrode surface which are relatively irreversible in that the reduction of a surface species (*e.g.*, an oxide) does not occur at the same electrode potential at which it is formed. This type of behaviour is again indicative of surface passivation effects and is frequently observed in the electro-oxidation of organics [9 - 11].

(c) Electrochemical reaction orders

In the study of the mechanism of an electrode reaction, an important diagnostic criterion is the order of the reaction. This parameter is especially useful for electrode processes proceeding in several steps, usually with the formation of adsorbed intermediates, *e.g.*, hydrogen evolution reaction [12, 13], anodic oxidation of ethylene glycol [14]. We have examined here the concentration-dependence, at a given electrode potential, of the rate of hydrazine oxidation, to obtain the reaction order derivative

$$\left(\frac{\partial \log i}{\partial \log \text{conc.}}\right)_E$$

The potentiostatic potential–log (current) relationships obtained on electrode # 3 (see Table 1) in 1M KOH solutions containing various concentrations of hydrazine are shown in Figs. 3 and 4 for the ascending and descending directions of potentials, respectively. From these data, one may extract the reaction order plot (Fig. 5) at an appropriate potential at which the Tafel lines are reasonably linear. The value of

$$\left(\frac{\partial \log i}{\partial \log \text{conc.}}\right)_E$$

observed is close to unity (Fig. 5).

It should be mentioned that a strictly valid reaction order plot should involve the concentration-dependence of exchange current densities, rather than the rate at a given potential. However, the extrapolation of Tafel regions to the measured or calculated reversible potentials needed to obtain exchange current densities is invalidated in the present case by the presence of hysteresis and inhibition effects in the potential–log (current) relations. Alternatively, the exchange currents cannot be measured directly near the reversible potential, owing to the presence of corrosion and parasitic reaction at the low anodic potentials, *viz.*, the "loop" below 0.1 V in Fig. 1. Since the lines in the Tafel regions in Figs. 3 and 4 are roughly parallel, our reaction plot (Fig. 5) does convey a valid dependence of the reaction rate on the concentration of hydrazine.

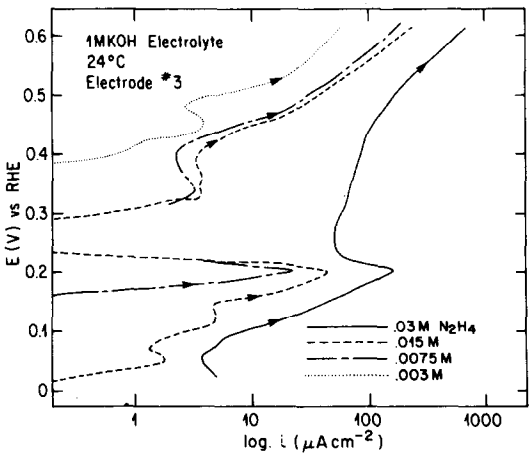

Fig. 3. Potentiostatic potential–log (current density) relationships in the ascending directions of potentials for various hydrazine concentrations; relevant experimental conditions shown in the Figure.

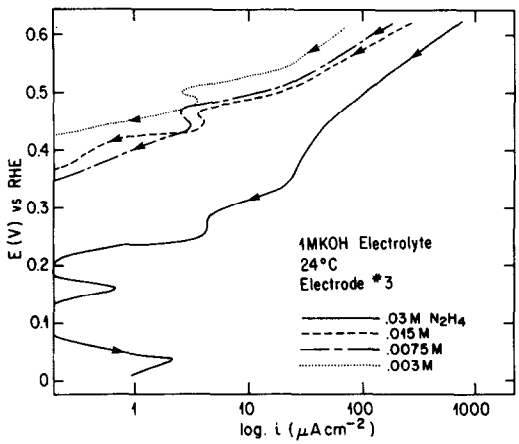

Fig. 4. As in Fig. 3, but for the descending directions of potentials.

In this connection, the slight differences in the appearance of the plots in Fig. 1, and in Figs. 3 and 4 (at the same concentration of hydrazine) need comment. In Fig. 1, the run was commenced at around the hydrogen potential, and the curve in the ascending direction of potential was thus obtained first, followed immediately by the one in the descending direction; this procedure reveals more "structure" in the curves. In Figs. 3 and 4, the reverse procedure was adopted in that the run was commenced at the higher anodic potential; this sequence gives more reproducible rates but less structure. The fundamental features, *e.g.*, the potentials of the inhibition inflexion and the magnitudes of the Tafel slopes, etc., are identical in all these curves, however.

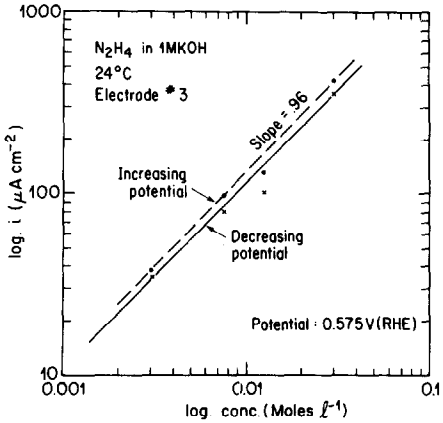

Fig. 5. The plots to determine the reaction order derivative, $(\partial \log i/\partial \log \text{conc.})_E$; the data for this Figure have been extracted from Figs. 3 and 4.

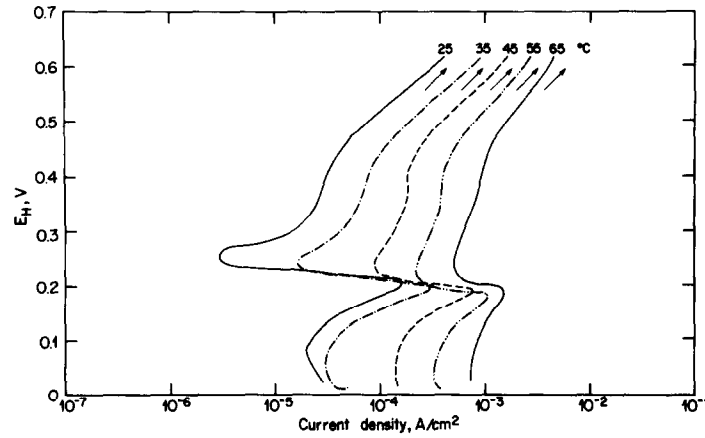

Fig. 6. Potentiostatic potential–log (current density) relationships on electrode # 3 (Table 1) in 1M KOH containing 0.1% hydrazine in ascending directions of potential and temperature, at the shown values of temperature.

(d) Temperature effects

The temperature-dependence of the reaction rate of an electrode process can, under favourable circumstances, provide some information on its mechanistic characteristics. The potentiostatic current–potential relationships for the anodic oxidation of hydrazine on electrode # 3 (see Table 1) were determined at several temperatures, both in the ascending (Fig. 6) and the descending (Fig. 7) direction of electrode potentials.

At a given potential, the rate increased with increasing temperature, as expected from theory [12]. These plots provide a means of determining the apparent heat of activation values at a given potential, *i.e.*, the derivative,

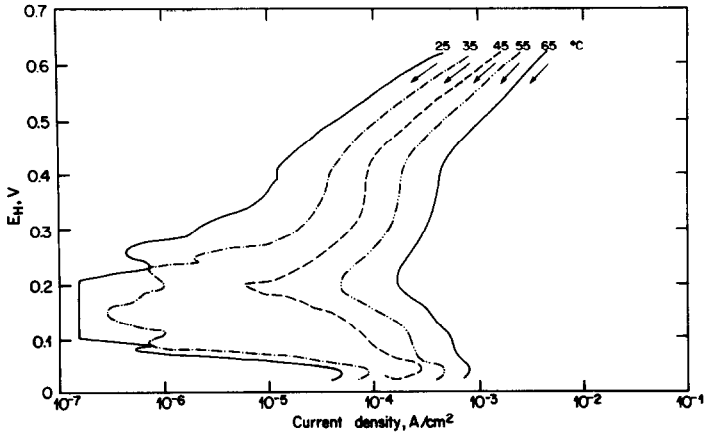

Fig. 7. As in Fig. 6, but in the descending directions of potential and temperature.

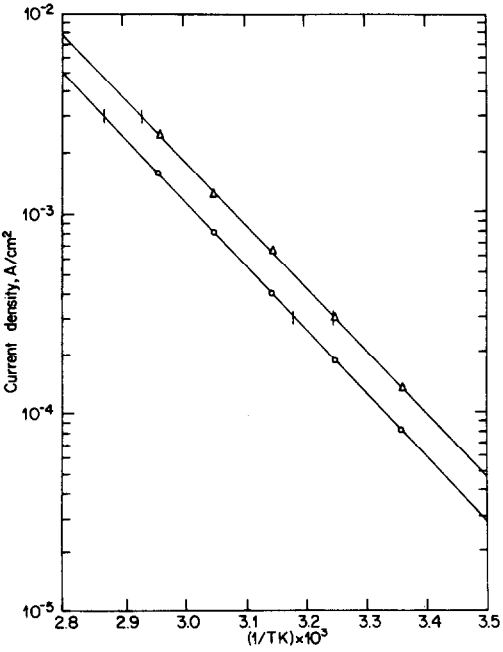

Fig. 8. The values of current densities at 0.526 V plotted against the corresponding $1/T$ values where T is the temperature in K. These data have been extracted from Figs. 6 (Δ) and 7 (o), respectively. The apparent heats of activation given by these plots are around 14.7 kcal mole^{-1}.

$$\left(\frac{\partial \log i}{\partial (1/T)}\right)_E$$

through a graph such as Fig. 8. This derivative, usually represented by ΔH^*, has a value around 15 kcal mole^{-1}, both for the ascending and the descending directions of potentials.

It should be noted that the apparent heats of activation at the reversible potential cannot be determined owing to the inaccessibility of the exchange current density values, for reasons mentioned in the Section on "Electrochemical reaction orders".

(e) Ellipsometric studies of the electrode surface

Figures 9 - 11 illustrate typical ellipsometric data. The phase retardation, Δ, calculated from the experimental azimuth (x) is plotted *versus* the scanning potential values for a Co cemented electrode with and without hydrazine, as well as for pure WC in the same conditions. In Fig. 9 we note the important changes brought about by a first polarization from 0.625 V (*vs.* RHE) to a cathodic potential value. The abrupt increase in the Δ value as the potential goes from 0.5 to 0.35 V corresponds to active dissolution of the Co, and can be associated with the anodic currents observed in this potential range in the first polarization curve. As the potential is returned to an anodic value (0.625 V) from 0.25 V, smaller variations in the ellipsometric parameter are observed, indicating that the changes brought about by the first polarization are not completely reversible. This situation is different from what is observed on noble metals such as Au or Pt [17, 18]. Similar data were recorded for the other ellipsometric parameters (ψ and the reflectivity). One outstanding feature noted on the second sweep is the minimal change in Δ values as the potentials are scanned from anodic to cathodic values. The only change observed from the cathodic return sweep illustrates a reversible phenomenon as the Δ value changes from 108.0° at 0.1 V in the cathodic scan to 108.7° at the same potential in the anodic scan, and the Δ changes in the first cathodic (from 0.625 to 0.25 V) potential sweep. As this first scan is completed the electrode surface remains unaffected by the

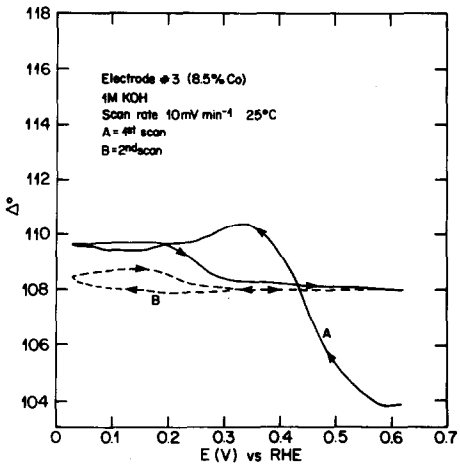

Fig. 9. The ellipsometer parameter Δ (in degrees) plotted *vs.* the electrode potential (E in V *vs.* RHE) for a cobalt-cemented carbide electrode (electrode # 3) in 1M KOH; potential scan rate 10 mV min^{-1}.

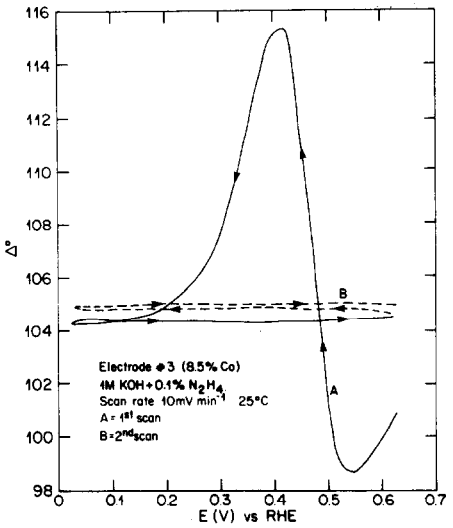

Fig. 10. The ellipsometer parameter Δ (in degrees) plotted *vs.* the electrode potential (E in V *vs.* RHE) for a cobalt-cemented carbide electrode (electrode # 3) in 1M KOH with 0.1% hydrazine; potential scan rate 10 mV min^{-1} for two potential scans.

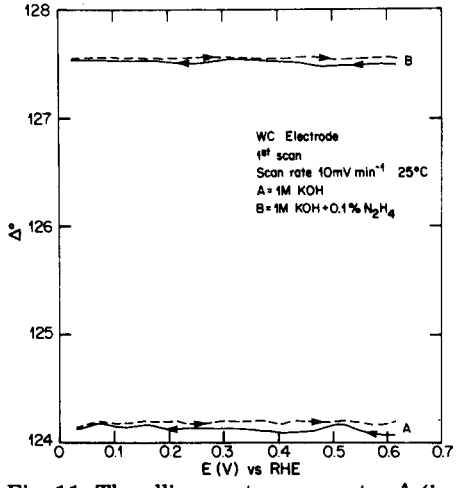

Fig. 11. The ellipsometer parameter Δ (in degrees) *vs.* the electrode potential (E in V *vs.* RHE) for a tungsten carbide electrode (electrode # 5) in 1M KOH with and without 0.1% hydrazine: first scan only at a scan rate of 10 mV min^{-1}.

potential scanning, illustrating the passive nature of the surface. Qualitatively similar behaviour is also observed in the presence of hydrazine (Fig. 10).

On WC no variations of the ellipsometric parameter are observed in respect of the number of scans or the presence of hydrazine, as shown in Fig. 11. We may also note the increased sensitivity of the Δ scale, indicating the inertness of the surface. The difference in the absolute values of Δ in the absence and presence of hydrazine is associated with the difference in position of the electrode during the two experiments.

Discussion

It appears convenient to commence the discussion of the mechanism of oxidation of hydrazine on cemented tungsten carbide electrodes by summarizing the salient features of the data presented here,

(1) The electrode surface is stabilized in KOH by the formation of a passive layer in the potential region used, as detailed in the Introduction. This is also suggested by the ellipsometric studies (Fig. 9).

(2) The value of the Tafel slope is *ca.* $2.3 \times 2RT/F$.

(3) The reaction order, $(\partial \log i/\partial \log \text{conc.})_E$, is equal to unity.

(4) The apparent heat of activation, ΔH^*, is quite high, *i.e.*, around 15 kcal as determined at an electrode potential of 0.526 V (RHE), as in Fig. 8. The kinetically significant ΔH^* value is the "true" ΔH^*, to be denoted by $(\Delta H^*)_{\text{true}}$ here; the two are related by ref. 15:

$$(\Delta H^*)_{\text{true}} = \Delta H^* + \beta\eta F + \beta\Delta H^\circ \qquad (1)$$

where ΔH^* is the value at a given E value (=0.526 V here); β is a symmetry factor, usually equal to 0.5; η is the overpotential for the hydrazine oxidation at the electrode potential used to determine ΔH^*; F is the Faraday constant; ΔH° is the enthalpy change in the single (half-cell) reaction of the oxidation of hydrazine.

Although the magnitude of factors $\beta\eta F$ and $\beta\Delta H^\circ$ could, in principle, be calculated through appropriate thermodynamic data, the quantitative figure thus obtained would have little validity in view of the uncertainty regarding the actual values of β for the present case; the invalidity is similar to the invalidity of extrapolating Tafel lines to the reversible potential to obtain exchange current densities in the present case, as discussed under "Results". However, qualitatively, it is quite clear from eqn. (1) that $(\Delta H^*)_{\text{true}}$ would be much higher than the ΔH^* value in Fig. 8. For the purposes of mechanistic discussion here, it may thus be stated that the anodic oxidation of hydrazine on cemented carbides proceeds with a very high heat of activation.

(5) There is no direct evidence for the deposition and the removal of adsorbed intermediate in the potentiodynamic profiles (Fig. 2).

Based on the detailed kinetic schemes examined by Conway *et al.* [16] for the anodic oxidation of hydrazine on platinum and the magnitude of electrode kinetic parameters observed in the present study, the following reaction pathway may be proposed:

$$2M + N_2H_4 \xrightarrow{\text{Chem}} M\text{–}N_2H_3 + M\text{–}H \qquad (2)$$

$$M\text{–}H \xrightarrow{\text{Instantaneous}} M + H^+ + e \qquad (3)$$

$$M\text{–}N_2H_3 + OH^- \xrightarrow{\text{r.d.s.}} M\text{–}N_2H_2 + H_2O. \qquad (4)$$

Here a chemical dissociative adsorption of N_2H_4 in step (2) is accompanied by the parallel instantaneous proton ionization in step (3) in a manner

that is not kinetically recognizable, as discussed previously [16]. This is followed by the rate-determining step (r.d.s.) shown in eqn. (4). The subsequent removal of $M-N_2H_2$ takes place through "fast" steps of the type

$$M-N_2H_2 \longrightarrow M-N_2H + H^+ + e \quad (5)$$

$$M-N_2H \longrightarrow M + N_2 + H^+ + e \quad (6)$$

or

$$M-N_2H_2 + OH^- \longrightarrow M-N_2H + H_2O \quad (5a)$$

$$M-N_2H + OH^- \longrightarrow M + N_2 + H_2O. \quad (6a)$$

It should be noted that steps (5) and (5a), as well as steps (6) and (6a) are kinetically indistinguishable.

The values of the Tafel slope ($2.3 \times 2RT/F$), reaction order ($\partial \log i / \partial \log \text{conc.})_E \approx 1$, and the apparent heat of activation at a given potential ($\Delta H^* = 15$ kcal mole^{-1}) are consistent with this rate-determining step. Also, an absence of the electrode coverage in the potentiodynamic profiles would be compatible with the first charge transfer (*i.e.*, kinetically-significant charge transfer) as the "slow" step, with subsequent steps removing the adsorbed species thus produced as the "fast" ones, as occurs in the above scheme. The oxide-covered passive electrode surface indicated here would be expected, in general, not to support a substantial steady-state coverage by an adsorbed species other than the surface oxide, in contrast to the case of platinum [16].

It should be noted that one cannot examine the reaction order with respect to the hydroxyl ions in order to obtain further information in support of (or in contradiction of) the above mechanism, since in the highly alkaline solutions used here, the concentration-dependence in hydroxyl ions would be expected to be pseudo-zero order.

Based on the results in Table 2, it would appear that one must propose a mechanism that does not involve the rupture of bonds, other than in the usually facile dehydrogenation; otherwise, it is not possible to suggest plausible reasons for the appreciable oxidation of hydrazine alone among all the compounds listed in Table 2. Such a mechanism has been proposed above. It should be added that the oxidation rate of biguanide shown in Table 2 does not appear to be the true oxidation rate in view of the visible corrosion of the electrode and the formation of a yellow precipitate on its surface, as pointed out in the "Introduction".

Conclusions

(1) Tungsten carbide electrodes cemented by cobalt show a good electrochemical stability in the potential range *ca.* 0.0 - 0.7 V (RHE) in strongly alkaline solutions. The presence of a passivating surface oxide is indicated.

(2) These electrodes show a pronounced activity towards the anodic oxidation of hydrazine, but not for several other model organic compounds.

(3) This activity is associated with the presence of cobalt in the electrodes since pure tungsten carbide is quite inactive.

(4) The electrode kinetic data on the oxidation of hydrazine on these electrodes indicate a mechanism in which the first charge transfer involving a hydroxyl ion and a molecular residue of hydrazine is the rate-determining step.

References

1 C. N. Smithell (ed.), *Metals Reference Book*, Butterworths, London, 1976, M 1262.
2 R. B. Levy and M. Boudart, *Science, 181* (1973) 547.
3 L. H. Bennet, J. R. Cuthill, A. J. McAlister, N. E. Erickson and R. E. Watson, *Science, 184* (1974) 563; *187* (1975) 858.
4 L. H. Bennet, A. J. McAlister, J. R. Cuthill and N. E. Erickson, *J. Mol. Catal., 2* (1977) 203.
5 P. N. Ross and P. Stonehart, *J. Catal., 39* (1975) 298.
6 F. Mazza and S. Trassati, *J. Electrochem. Soc., 110* (1963) 847.
7 M. Svata and S. Rudolf, *J. Power Sources, 1* (1976 - 1977) 277.
8 A. K. Vijh, *J. Catal., 37* (1975) 410.
9 A. K. Vijh, *Electrochemistry of Metals and Semiconductors*, Marcel Dekker, New York, 1973.
10 D. Gilroy and B. E. Conway, *J. Phys. Chem., 69* (1965) 1259.
10a K. V. Benda, H. Binder, W. Faul and G. Sandstede, *Chem. Ing. Tech., 43* (1971) 1223.
11 A. K. Vijh and B. E. Conway, *Chem. Rev., 67* (1967) 623.
12 B. E. Conway, *Theory and Principles of Electrode Processes*, Ronald Press, New York, 1965.
13 A. K. Vijh, *J. Phys. Chem., 72* (1968) 1148.
14 A. K. Vijh, *Can. J. Chem., 49* (1971) 78.
15 B. E. Conway and D. J. MacKinnon, *J. Electrochem. Soc., 116* (1969) 1665.
16 B. E. Conway, N. Marincic, D. Gilroy and E. J. Rudd, *J. Electrochem. Soc., 113* (1966) 1144.
17 R. Greef, *J. Chem. Phys., 51* (1969) 3198.
18 Y. Y. Vinnikov, V. A. Shepelin and V. I. Veselouskii, *Elektrokhimiya, 8* (1972) 1229.